DOI: 10.1021/ma902323t

Macromolecules
ARTICLE

Evidence of Temperature-Induced Subdiffusion of Water on the Micrometer Scale in a Nafion Membrane

Cinzia Casieri,[†] Antonina Monaco,[‡] and Francesco De Luca*[,‡]

[†]*INFM-CRS SOFT and Dipartimento di Fisica, Università de L'Aquila, V. Vetoio 10, I-67010 Coppito, L'Aquila, Italy and* [‡]*INFM-CRS SOFT and Dipartimento di Fisica, Università 'Sapienza', P.le A. Moro 2, I-00185 Roma, Italy*

Received October 19, 2009; Revised Manuscript Received December 4, 2009

ABSTRACT: To investigate the topological features of proton transport in perfluorosulfonic membranes, we performed time-dependent ^{1}H NMR pulsed gradient spin−echo experiments on four samples of Nafion-115 with $\lambda = 0.5$, 3.2, 5.8, and 12.4 water molecules per sulfonic group at different temperatures ranging from 278 to 348 K. A subdiffusive behavior of water, $< z^2 > = 2D_\alpha t^\alpha$ with $0.75 < \alpha < 1$, was observed above 320 K for each of the four samples. The onset of water subdiffusion with increasing temperature, basically independent of membrane hydration, supports the hypothesis of a drop in dimensionality for the diffusion space. Diffusion−diffraction effects on the NMR echo-signal attenuation confirm that proton displacement is restricted because of an interconnected pore structure with a coherence length of ~1 μm, which depends on temperature and water content.

I. Introduction

Perfluorosulfonate ionomer membranes, such as Nafion, are currently used as electrode separators in fuel cells and have been studied for decades.[1,2] According to the Grotthuss mechanism, Nafion has a high proton conductivity, which is strongly affected by temperature and by the state of hydration of the membrane itself.[3−6] Although a detailed model for the structure of Nafion is still a work in progress, its hydrated structure is effectively represented by the Gierke cluster network model: a system of channels that connect cavities called ionic clusters, each having sulfonic groups ($-SO_3H$) located on its external surface, which extends into the cavity and forms reverse-micelle-like structures.[7] More recently, new structural models have been proposed. One model describes the Nafion membrane as an aggregation of polymeric chains forming elongated objects embedded in a continuous ionic medium.[8] On larger scales, these aggregates form bundles characterized by an orientational order between the aggregates themselves.[8] Another model suggests parallel, but otherwise randomly packed, water channels surrounded by a polymer shell, forming inverted-micelle cylinders.[9] Irrespective of which model could best represent water−polymer microphase separation, a full description is not yet available, especially concerning how the morphology and topology of hydrated membranes may influence proton transport. It is known that to allow proton conduction by Grotthuss mechanism, the aqueous phase must form hydrogen bonds paths through the membrane. Two major elements contribute to the formation of a connected network of water clusters inside the membrane, that is, the amount of water in the membrane and the multiscale structure of the polymer network.

This work aimed to a better understanding of the long-range (micrometer-scale) diffusion space of water in the polymeric membrane as well as of its behavior under different water content and temperature conditions.

*To whom correspondence should be addressed. E-mail: francesco.deluca@roma1.infn.it.

Nuclear magnetic resonance (NMR) spectroscopy represents an effective and low-perturbing tool for measuring the transport of NMR-sensitive nuclei in diamagnetic or quasi-diamagnetic systems. In the pulsed-gradient spin−echo (PGSE) method,[10] two magnetic field-gradient pulses are used to label the starting and final space positions of nuclear spins that spread around during the time interval (Δ) separating the two pulses. Δ works as a flying time for spins characterized by a phase term $\mathbf{q}\cdot\mathbf{r} = \gamma\delta\mathbf{g}\cdot\mathbf{r}$, where $\mathbf{q}$ plays the role of a dynamic wave vector, which depends on the proton gyromagnetic ratio, γ, the duration of the gradient pulse, δ, and the gradient vector, $\mathbf{g}$. In real systems, the NMR echo signal, $E(\mathbf{q},\Delta)$, is a superposition of coherent spin states in which each $\exp[i\mathbf{q}(\mathbf{r}'(\Delta) - \mathbf{r}(0))]$ term is weighted by the probability for a spin to be at $\mathbf{r}$ at $t = 0$ and diffuse toward $\mathbf{r}'$ (i.e., to shift of $\mathbf{R} = \mathbf{r}'(\Delta) - \mathbf{r}(0)$) during Δ.

The time-dependent PGSE experiment, in the limit $\delta \ll \Delta$, provides a direct assessment of the time evolution of the mean square displacement of spins by means of the echo-signal attenuation

$$< R^2(\Delta) > = -6\, ln[E(q,\Delta)/E(0,\Delta)]/q^2 \qquad (1a)$$

By analogy to scattering methods, the wave vector $\mathbf{q}$ can be regarded as a probe of the reciprocal space of spin displacements; at small q values, the experiment probes diffusion behavior on the long-distance scale.

In ordinary isotropic unrestricted diffusion, the displacement distribution is a Gaussian function, and the mean square displacement, $< R^2 >$, is expressed in terms of the scalar self-diffusion coefficient D, as $< R^2 > = 6Dt$.[11] A deviation from the Gaussian distribution appears when "soft" geometrical constraints reduce the dimensionality of the volume where spins are diffusing. When solvent molecules are obliged to diffuse along lamellae in a multidomain lyotropic liquid crystal or a random-coil polymer molecule is moving in the topological constraints due to neighboring polymers, they exhibit "softer" restrictions to their motion (than hard geometrical confinement suffered by water in the porous space of a rock), which have the effect of

 Published on Web 12/11/2009

limiting the distribution of translational displacements as the flight time gets larger.[10] That is the so-called "anomalous diffusion", and $< R^2 >$ can be expressed as a power law

$$< R^2 > = 6D_\alpha t^\alpha \quad (1b)$$

where the generalized diffusion coefficient D_α has the physical dimension $[D_\alpha] = [\text{length}]^2/[\text{time}]^\alpha$. According to the value of the exponent α, one usually distinguishes several regimes of anomalous transport.[12] In what follows, the attention will be directed to subdiffusive phenomena, which correspond to $0 < \alpha < 1$. Diffusion on random-site percolation clusters is an example of subdiffusive behavior: the time dependence of the mean square displacement is represented by $\alpha = 0.75$.[13,14]

For representing the anomalous evolution of mean square displacements in Nafion, a different formalism has been recently introduced that makes use of an apparent diffusion coefficient, $< R^2 > = 6D_{app}t$.[15,16] Because the NMR technique gives us a chance to measure directly the $< R^2 >$ value for each diffusion time, we can easily use eq 1b to better highlight the topological properties of the diffusion volume of our samples via the α index. To be more precise, as NMR diffusion experiments are performed with unidirectional field gradients, only one component of $< R^2 >$, that is, $< z^2 >$, is probed. Eqs 1a and 1b then become

$$< z^2(\Delta) > = -2\, ln[E(q,\Delta)/E(0,\Delta)]/q^2 \quad (2a)$$

$$< z^2 > = 2D_\alpha t^\alpha \quad (2b)$$

In recent years, subdiffusion has received much of attention because it seems to emerge in a large variety of complex systems dominated by slow processes.[11] Subdiffusive dynamics has been associated with systems belonging to various scientific areas, ranging from physics (glassy dynamics,[17] charge transport in amorphous semiconductors,[18] polymer dynamics in porous materials)[19] to biology (cytoplasmatic crowding in living cells,[20] dynamics of biomolecule networks).[21]

When the displacement occurs within a confining geometry, its distribution function becomes non-Gaussian, and the PGSE signal is able to yield further information on the structure surrounding the molecular probe. A diffraction-like pattern appears in the PGSE signal decay owing to the constructive interference between signals of spins migrated into different sites: if Δ is long enough, then a coherence peak occurs when **q** matches the length scale of the mean spacing between sites.[22]

In this study, PGSE signals were collected using different **q** and Δ values, at different temperatures, and at different degrees of hydration of Nafion to get space and time encoding of water diffusion on the millisecond and micrometer scales. This is the scale that characterizes the size of and the spacing between ionic domains, and these issues must be well understood to account for a percolation topology, which is expressed in terms of measured ionic conductivities and diffusion coefficients.

II. Experimental Section

Nafion-115 membranes, with a nominal equivalent weight of 1100 per sulfonic group and a thickness of about 130 μm, were purchased from Aldrich. The membranes were treated to remove impurities and cut to obtain rectangular strips of about 2×4 mm^2.[23] The strips were stored in four NMR glass tubes and kept at about 0, 20, 70, and 100% relative humidity. After equilibrium was reached (a few days), the glass tubes were doubly sealed with silicone rubber plugs to prevent change in water content during measurements. H_2O contents, calculated from the weight loss observed after heating the strips for 15 h under vacuum at 120 °C, correspond to ratios (λ) of water molecules per $-SO_3H$ group of 0.5, 3.2, 5.8, and 12.4, respectively. The Nafion strips were oriented randomly inside the NMR tubes for them to turn out randomly oriented with respect to both the main NMR magnetic field and magnetic field gradients.

^{1}H-PGSE experiments were performed by means of a Bruker Avance 300 MHz spectrometer equipped with high-intensity gradients that allow high q values to be reached. In particular, the z-gradient unit used in the present experiment generates a maximum gradient strength of ~1100 G/cm. A stimulated-echo radio frequency pulse sequence[10] was used with 32 gradient steps, from 0 to 650 G/cm, with a gradient-pulse length of $\delta = 1.5$ ms. This means that $< z^2 >$ was measured with 32 different q values at each fixed Δ. The Δ interval spanned 20 different values, ranging from 4 to 100 ms. For each sample, all sets of Δ-dependent experiments were performed in the temperature range 278−348 K at a step of 10 K.

We calibrated gradient strength by measuring, at 298 K, ^{1}H self-diffusion coefficients of bulk octan-1-ol ($D = 1.4 \times 10^{-6}$ cm^2/s) and bulk glycerol ($D = 2.0 \times 10^{-8}$ cm^2/s) to cover a large interval of D values. The test was performed using all of the above-mentioned Δ values. The calibration factor was obtained by fitting the echo signal, taken as a function of the wave vector, with the Stejskal−Tanner formula:[24] $E_\Delta(q) = E_\Delta(0)\exp(-q^2D(\Delta - \delta/3))$. The effective diffusion time ($\Delta - \delta/3$) will be hereafter indicated as Δ_{eff}. According to results, we were able to assume that for self-diffusion data obtained for glycerol and octan-1-ol, the time-dependent behavior can be considered to be reliable (within a 10% error) over the full experienced Δ range.

III. Results and Discussion

In Figure 1A, an example ($\lambda = 12.4$ and $T = 278$ K) of the Δ evolution of the PGSE signal attenuation data against q^2 is shown. To highlight how the effective diffusion time influences the overview of the diffusion phenomena, in Figure 1B, the same data are plotted against $q^2\Delta_{eff}$. At short Δ values, the ordinary as

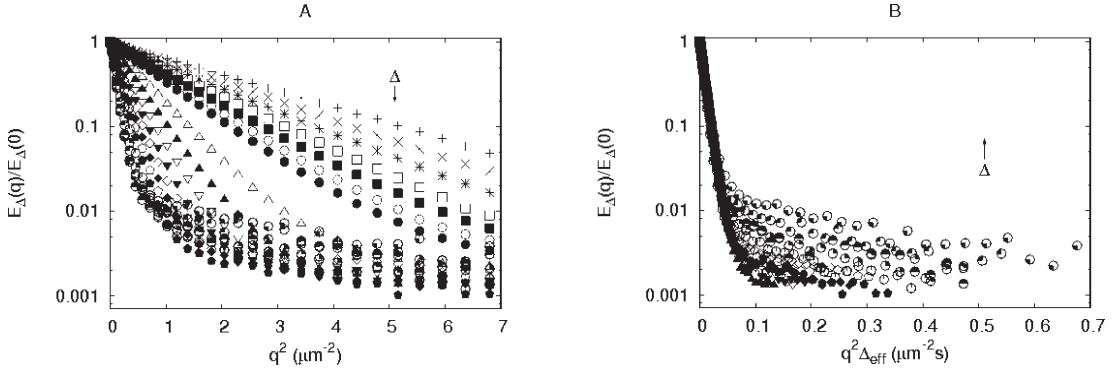

Figure 1. (A) Echo−signal attenuation, $E_\Delta(q)/E_\Delta(0)$, versus square wave vector for the sample with $\lambda = 12.4$ at $T = 278$ K. Data are shown for the full performed set of diffusion times, Δ, ranging from 4 (upper curve) to 100 ms (lower curve). (B) As in part A, but with data plotted against $q^2\Delta_{eff}$, where Δ_{eff} is the effective diffusion time.

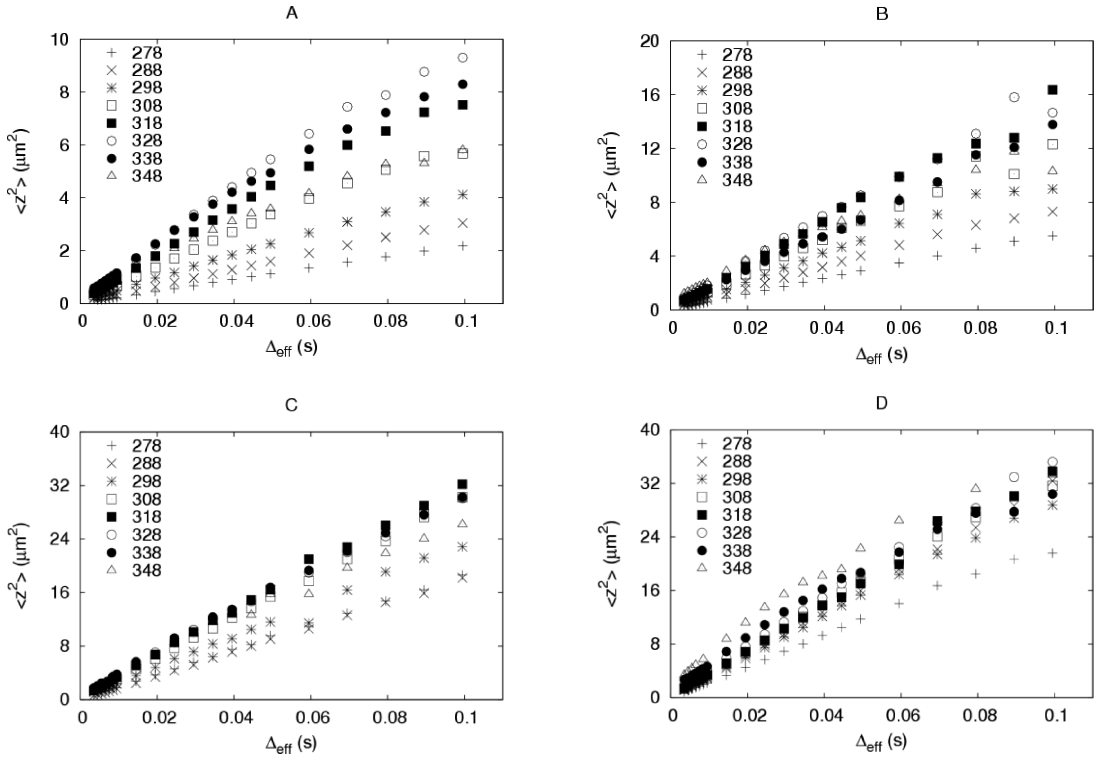

Figure 2. Mean square displacement along the gradient axis, $<z^2>$, versus effective diffusion time Δ_{eff} for samples with λ = (A) 0.5, (B) 3.2, (C) 5.8, and (D) 12.4. Data are shown for the full performed set of temperatures in the range of 278−348 K.

well as anomalous diffusion regime shows a linear behavior of the PGSE attenuation, whereas at higher Δ values and large enough **q** values, a restricted diffusion regime appears, which manifests itself as a nonlinear behavior of the echo attenuation.[10]

As pointed out in the Introduction, this is expected because the single water molecule explores larger space structures over larger Δ values.[22,25]

According to eq 2a, the mean square displacements, for each Δ, have been obtained by fitting the PGSE signal as a function of the square wave vector, q^2.[10] To pay attention to the onset of effects that modify "free" diffusion, at short values of Δ, the mean square displacement has been evaluated by considering the full decay of the echo amplitude versus q^2, whereas, at higher Δ values, this parameter has been estimated by the decay of the echo amplitude versus small q^2 values only (∼95% of the full decay amplitude).

In Figure 2, the $<z^2>$ values versus the effective diffusion time, Δ_{eff}, are shown for samples with λ = (A) 0.5, (B) 3.2, (C) 5.8, and (D) 12.4 at all temperatures.

At low temperatures, the displacement grows quite regularly with time, whereas, at higher T values, it is evident that $<z^2>$ tends to values that are lower than analogous values reached at lower temperatures for the same Δ_{eff}. To test the time dependence of displacements on temperature, a log−log scale is used to plot $<z^2>(\Delta_{eff})$ data. In Figure 3, $<z^2>(\Delta_{eff})$ is reported for λ = 12.4 only, at T = 348 (▲), 328 (■), and 278 K (●).

The fairly well linear behavior shown by the experimental data points out the reliability of the experimental setup. The lines represent the best fits to eq 2b for the evaluation of D_α and α. The results of this procedure are summarized in Figure 4, where the full evolution in temperature of the α index for the four samples with λ = 0.5 (○), 3.2 (quarter-closed circles), 5.8 (◐), and 12.4 (●) is shown.

At low temperatures, up to ∼320 K, all $<z^2(\Delta_{eff})>$ values are characterized by an exponent α ≅ 1. Above this temperature, $<z^2(\Delta_{eff})>$ values are marked, for each sample, by a decrease in

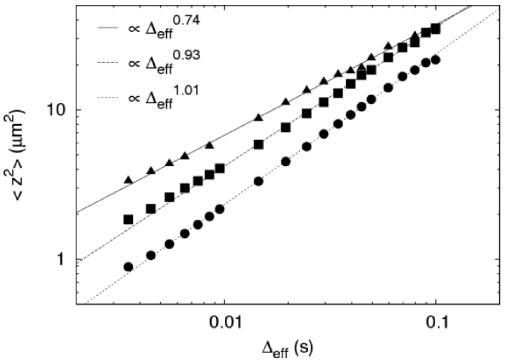

Figure 3. On a log−log scale, mean square displacement along the gradient axis, $<z^2>$, versus effective diffusion time, Δ_{eff}, for the sample with λ = 12.4 at T = 348 (▲), 328 (■), and 278 K (●). The lines are the best fits of data to the function $<z^2> = 2D_\alpha\Delta_{eff}^{\alpha}$.

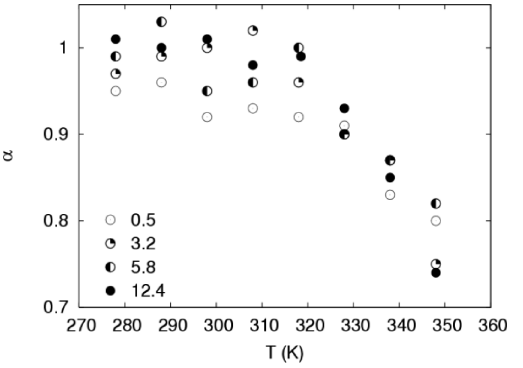

Figure 4. Time-scaling exponent, α, versus temperature, T, for samples with λ = 0.5 (○), 3.2 (quarter-closed circles), 5.8 (◐), and 12.4 (●).

the α index, which is a clear sign of a progressive increase in the subdiffusive behavior of water with T, which is essentially

independent of the hydration level of the membranes. As a consequence of the long-range tortuousity of diffusion pathways,[16] which may increase as temperature gets higher, the membrane is likely approaching a topological modification that supports a percolation regime for the translational dynamics of water.

The mechanism of subdiffusion cannot be in fact associated with a change in the coupling modes of water with sulfonic groups because such an effect would appear at temperatures < 320 K as well, not to mention the fact that at low temperatures the coupling of water with sulfonic groups should be more effective because of the lower thermal energy of water itself. The dependence of the onset of subdiffusion on temperature is a sign of a change in the Nafion topology that modifies the space dimensionality. At T = 348 K, the limit value of the $<z^2(\Delta_{eff})>$ exponent is $\alpha \cong 0.75$ for all samples: this supports the model of diffusion on random-site percolation clusters.[16] The present results, therefore, support the idea that a percolation regime can be induced by temperature via a topological modification of the polymer that does not involve, or scarcely involves, water content. It could be supposed that by increasing the temperature of the membrane, the connectivity either among ionic clusters or among water channels reduces because of an increase in thermal fluctuations; furthermore, above a specific temperature ($T \approx$ 320 K), the onset of a percolative dynamics for water seems to appear, which means that water is likely to diffuse within clusters of connected clusters, following a scheme characterized by self-similarity properties (the limit $\alpha = 0.75$ corresponds to a fractal dimension $d = 2$). This mechanism appears to be basically independent of water density.

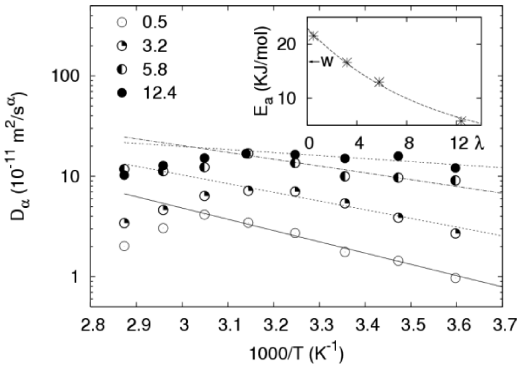

Figure 5. Generalized diffusion coefficient, D_α, versus temperature, T, for samples with λ = 0.5 (○), 3.2 (quarter-closed circles), 5.8 (◐), and 12.4 (●). The lines are the best fits of data to the Arrhenius law. The evaluated activation energy, E_a, versus the hydration degree of the membrane, λ ([H_2O]/[$-SO_3H$]), is shown in the inset. The line is the best fit of data to an exponential function; the arrow points to the value for bulk water as a reference.

Results about the generalized diffusion coefficient are reported in Figure 5, where D_α is plotted against T.

The diffusion activation energy (look at the inset in Figure 5), which can be assessed over the temperature range where α is temperature-independent ($\alpha \cong 1$), is found to be >17 kJ/mol (value for bulk water) for water contents lower than the one required for almost primary hydration of the sulfonic group $\lambda \cong$ 3, which is in agreement with an early evaluation.[5] But, unlike the same study, E_a progressively decreases for $\lambda > 3$, and this seems to be due to a high molecular rotational motion rather than a bulk-water-like behavior.[26] In the inset, the diffusion activation energy against water content (expressed by λ) shows an exponential behavior ($E_a \propto \exp(-\lambda/10)$) with a characteristic constant that is very close to the one we have evaluated from activation energy for conductance by Cappadonia data on Nafion-117 ($E_a^C \propto \exp(-\lambda/9)$).[4] Where our results trace out the Arrhenius regime, water self-diffusion is strictly related to the behavior of proton conductivity with respect to water content.[4,5]

Beyond the temperature range held true for the Arrhenius regime, the comparison between diffusion and conduction behaviors needs a deeper discussion in light of a modification of the membrane network for proton transport, which is emphasized by our results. Interesting results show that when relative humidity is held constant, water uptake[27] and conductivity[28] remain constant at high temperatures, above ~80 °C. It has been suggested that as temperature increases, the expected increase in conductivity is balanced by a change in the membrane microstructure that reduces mobility. The same behavior can be deduced from a more recent report[6] as well. According to our results, the onset of anomalous diffusion above 320 K may be an early sign of this microstructure change.

In Figure 6, some examples of the PGSE signal attenuation versus the dynamic wave vector are reported for different Δ values at T = 278 (Figure 6A) and 348 K (Figure 6B) for λ = 12.4.

Diffraction phenomena are evident and are more pronounced in the PGSE signal decays at Δ = 100 ms. The arrows indicate the diffraction-like peaks at $q = 1.17$ (T = 278 K) and 0.78 μm^{-1} (T = 348 K) corresponding to a structure with a coherence length of ~0.9 and ~1.3 μm, respectively. Full data are reported in Table 1.

Even in complex systems such as Nafion, where geometric confinement sites (ionic clusters or channels) may be interconnected with random orientations, the NMR signal suffers from interference effects between distant structures because of the long-range migration of molecules over the diffusion time scale.

This effect in Nafion is well measurable at high T and high hydration degree of the membrane; otherwise, the slow diffusion

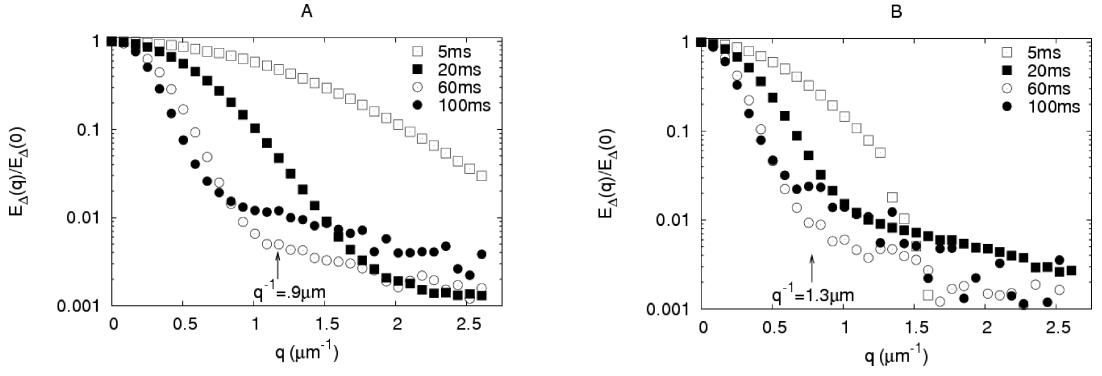

Figure 6. Echo-signal attenuation, $E_\Delta(q)/E_\Delta(0)$, versus dynamic wave vector q for the sample with λ = 12.4 at T = (A) 278 and (B) 348 K. Data are shown for a few selected diffusion times: 5 (□), 20 (■), 60 (○), and 100 ms (●). A coherence peak appears at large diffusion times, corresponding to a spatial coherence length q^{-1} of (A) 0.9 and (B) 1.3 μm.

Table 1. Length Scale of the Structure Mean-Spacing of the Membrane, Expressed in Micrometers, Evaluated from the Diffraction Effects on Echo-Signal Decays Acquired at Large Diffusion Times for All Samples at All Temperatures

T (K)	278	288	298	308	318	328	338	348
$\lambda = 0.5$	0.6	0.6	0.8	0.8	0.9	1.0	1.0	0.9
$\lambda = 3.2$	0.7	0.8	0.9	0.9	1.0	1.1	1.0	1.0
$\lambda = 5.8$	0.9	0.9	1.0	1.0	1.0	1.1	1.1	1.0
$\lambda = 12.4$	0.9	1.1	1.0	1.1	1.2	1.3	1.3	1.3

motion inhibits the cumulative interference effects for single molecules between distant sites. Anyway, at $T = 278$ and 348 K, the structure length scale tends to grow slowly with the degree of hydration ($\lambda = 0.5$, 3.2, 5.8, and 12.4) in the ranges $0.6 < q^{-1} < 0.9$ and $0.9 < q^{-1} < 1.3$ μm, respectively.

To summarize data in Table 1, we may reasonably affirm that the hydration degree as well as the temperature tend to increase the length scale characterizing the long-range structure of Nafion. We cannot disregard the poor signal-to-noise ratio of the diffusion−diffraction effects, which is due to the extreme randomness of the diffraction pattern; nonetheless, in our opinion, the goodness of results is confirmed by their reproducibility under the same experimental conditions and by their regular behavior as the hydration degree of the membrane and temperature are increased. Moreover, the plot of this length scale against water content shows a rough linear behavior for all temperatures, with an angular coefficient that is close to the one we have evaluated from Bragg spacing by SAXS data on Nafion.[29] Therefore, the superstructure expansion on the micrometer scale with increasing water content, identified by NMR diffraction, seems to be related directly to a channel expansion on the nanoscale. As for the investigated behavior in temperature, our data do not represent a reliable source to extract any hypothetical second-order effect triggered by temperature and correlated to the above-mentioned micrometer-scale topological rearrangement: this is due to the poor quality of diffusive diffraction phenomena. Anyway, the increase in the length scale assessed from our data with increasing temperature appears to slow down at higher temperatures (in correspondence to the onset of subdiffusion), which is also suggested by recent SAXS profiles in temperature[30] in the range of 313−353 K.

These experimental evidence confirm early results about the existence of a superstructure on the micrometer scale in Nafion.[16,31] As far as we know, however, it is the first time that direct evidence about dependence on water content and temperature is given.

IV. Conclusions

NMR diffusometry can be used to characterize the probe motion (protons, as well as atoms, with nonzero nuclear spin) on the millisecond and micrometer scales. The long-range water transport through a perfluorosulfonate ionomer membrane depends on the long-range morphology on the dimensional scale investigated by the time-dependent ^{1}H-PGSE technique. The echo-signals must be collected with different q and/or Δ values to produce a proper space and time encoding of the diffusion volume. The experiments were performed on Nafion-115 at different hydration degrees and temperatures. Four samples with $\lambda = 0.5$, 3.2, 5.8, and 12.4, respectively, were considered at various temperatures ranging from 278 to 348 K.

By plotting the mean square displacement versus the effective diffusion time, as shown in Figure 3, a power law has been identified, which connects the mean square displacement to the "generalized diffusion coefficient" and to the diffusion evolution-time exponent: $<z^2> = 2D_\alpha t^\alpha$. As reported in Figure 4, a drop in dimensionality for the diffusion space has been deduced above ~320 K for all four samples by means of the time-scaling exponent. Moreover, the generalized diffusion coefficient versus temperature (Figure 5) is characterized by a linear behavior in the same range where $\alpha \cong 1$. Assuming that the Arrhenius law holds in this temperature range, it has been possible to discuss the activation energy behavior with respect to water content and to compare, at high temperatures, proton transport conductivity with proton diffusion.

Finally, clear and direct experimental evidence (Figure 6) of the existence of a superstructure on the micrometer scale has been given. The length scale is characterized by a slow increase in temperature and hydration level of the membrane.

Acknowledgment. We are indebted to Prof. M. Casciola (Università di Perugia) for supplying us with the experimental samples and to Prof. G. Onori (Università di Perugia) for introducing us to the topic of Nafion.

References and Notes

(1) Mauritz, K. A.; Moore, R. B. *Chem. Rev.* **2004**, *104*, 4535–4585.
(2) Kreuer, K. D.; Paddison, S. J.; Spohr, E.; Schuster, M. *Chem. Rev.* **2004**, *104*, 4637–4678.
(3) Zawodzinski, T. A., Jr.; Neeman, M.; Sillerud, L. O.; Gottesfeld, S. *J. Phys. Chem.* **1991**, *95*, 6040–6044.
(4) Cappadonia, M.; Erning, J. W.; Saberi Niaki, S. M.; Stimming, U. *Solid State Ionics* **1995**, *77*, 65–69.
(5) Kreuer, K. *Solid State Ionics* **1997**, *97*, 1–15.
(6) Ochi, S.; Kamishima, O.; Mizusaki, J.; Kawamura, J. *Solid State Ionics* **2009**, *180*, 580–584.
(7) Hsu, W. Y.; Gierke, T. D. *J. Membr. Sci.* **1983**, *13*, 307–326.
(8) Rubatat, L.; Gebel, G.; Diat, O. *Macromolecules* **2004**, *37*, 7772–7783.
(9) Schmidt-Rohr, K.; Chen, Q. *Nat. Mater.* **2008**, *7*, 75–83.
(10) Callaghan, P. T. *Principles of Nuclear Magnetic Resonance Microscopy*; Oxford University Press: New York, 1991.
(11) Metzler, R.; Klafter, J. *Phys. Rep.* **2000**, *339*, 1–77.
(12) Kimmich, R. *NMR Tomography, Diffusometry, Relaxometry*; Springer-Verlag: Berlin, 1997.
(13) Gefen, Y.; Aharony, A.; Alexander, S. *Phys. Rev. Lett.* **1983**, *50*, 77–80.
(14) Klemm, A.; Metzler, R.; Kimmich, R. *Phys. Rev. E* **2002**, *65*, 021112-1–021112-12.
(15) Zhang, J. H.; Giotto, M. V.; Wen, W. Y.; Jones, A. A. *J. Membr. Sci.* **2006**, *269*, 118–125.
(16) Ohkubo, T.; Kidena, K.; Ohira, A. *Macromolecules* **2008**, *41*, 8688–8693.
(17) *Measures of Complexity*; Peliti, L., Vulpiani, A., Eds.; Springer: Berlin, 1988.
(18) Scher, H.; Montroll, E. W. *Phys. Rev. B* **1975**, *12*, 2455–2477.
(19) Fischer, E.; Kimmich, R.; Beginn, U.; Moller, M.; Fatkullin, N. *Phys. Rev. E* **1999**, *59*, 4079–4084.
(20) Golding, I.; Cox, E. C. *Phys. Rev. Lett.* **2006**, *96*, 098102−1–098102−4.
(21) Wong, I. Y.; Gardel, M. L.; Reichman, D. R.; Weeks, E. R.; Valentine, M. T.; Bausch, R. A.; Weitz, D. A. *Phys. Rev. Lett.* **2004**, *92*, 178101−1–178101−4.
(22) Callaghan, P. T.; Coy, A.; Mac Gowan, D.; Packer, K. J.; Zelaya, F. O. *Nature* **1991**, *351*, 467–469.
(23) Paciaroni, A.; Casciola, M.; Cornicchi, E.; Marconi, M.; Onori, G.; Pica, M.; Narducci, R. *J. Phys. Chem. B* **2006**, *110*, 13769–13776.
(24) Stejskal, E. O.; Tanner, J. E. *J. Chem. Phys.* **1965**, *42*, 288–292.
(25) Callaghan, P. T.; Codd, S. L.; Seymour, J. D. *Concepts Magn. Reson.* **1999**, *11*, 181–202.
(26) Paddison, S. J.; Reagor, D. W.; Zawodzinski, T. A. *J. Electrochem. Soc.* **2000**, *147*, 617–626.
(27) Hinatsu, J. T.; Mizuhata, M.; Takenaka, H. *J. Electrochem. Soc.* **1994**, *141*, 1493–1498.
(28) Alberti, G.; Casciola, M.; Massinelli, L.; Bauer, B. *J. Membr. Sci.* **2001**, *185*, 73–81.
(29) Gierke, T. D.; Munn, G. E.; Wilson, F. C. *J. Polym. Sci., Polym. Phys.* **1981**, *19*, 1687–1704.
(30) Takimoto, N.; Wu, L.; Ohira, A.; Takeoka, Y.; Rikukawa, M. *Polymer* **2009**, *50*, 534–540.
(31) Kim, M.; Glinka, C. J.; Grot, A.; Grot, W. G. *Macromolecules* **2006**, *39*, 4775–4787.